

Machine learning-based prediction of cross-shore profile evolution in the southeastern Baltic Sea, Lithuania

Pranciškus Brazdžiūnas*, Darius Jarmalavičius, Gintautas Žilinskas, Donatas Pupienis

Brazdžiūnas, P., Jarmalavičius, D., Žilinskas, G., Pupienis, D. 2025. Machine learning-based prediction of cross-shore profile evolution in the southeastern Baltic Sea, Lithuania. *Baltica* 38 (2), 194–208. Vilnius. ISSN 1648-858X.


Manuscript submitted 6 June 2025 / Accepted 21 November 2025 / Available online 15 December 2025

© Baltica 2025

Abstract. This study explores the use of neural network-based machine learning techniques to predict yearly changes of the foredune height, beach height, and beach width. The research focuses on the evolution of the Curonian Spit coast based on cross-shore profile long-term field measurements (1993 to 2018) supported by the analysis of empirical and modelled annual wind, wave, and sea level data. The performance of two types of recurrent neural network models – LSTM and GRU – was assessed by monitoring training progress and validating on unseen data. Both demonstrated the ability to predict general trends; however, the LSTM model exhibited a superior performance in accurately discerning the direction of cross-shore profile parameters development. However, the models showed limited accuracy in predicting more stable morphometric parameters, such as foredune height, likely due to constrained variability in the available data. The signs of overfitting observed during training further highlight the insufficiency in both the variability and duration of the training data set. The findings demonstrate a high potential of machine learning methods to support coastal change forecasting, although the effectiveness of these models remains highly dependent on the quality, temporal span, and spatial coverage of the input data. Incorporating a longer time series with additional factors, such as nearshore seabed morphology and sediment type, may further enhance model performance.

Keywords: beach; foredune; coastal morphology; field surveys; algorithm

Pranciškus Brazdžiūnas* (pranciskus.brazdziunas@chgf.stud.vu.lt),

Donatas Pupienis (donatas.pupienis@gf.vu.lt),  <https://orcid.org/0000-0002-7310-70900>;

Vilnius University, Faculty of Chemistry and Geosciences, Institute of Geosciences, Čiurlionio Str. 21/27, LT-03101 Vilnius, Lithuania;

Darius Jarmalavičius (darius.jarmalavicius@gamtc.lt),  <https://orcid.org/0000-0002-5885-9366>,

Gintautas Žilinskas (gintautas.zilinskas@gamtc.lt);

State Scientific Research Institute Nature Research Centre, Laboratory of Geoenvironmental Research, Akademijos Str. 2, LT-08412, Vilnius, Lithuania

*Corresponding author

INTRODUCTION

The coastal zone is one of the most dynamic elements of the geographical environment, undergoing continuous transformation due to climate change, sea level rise, storm activity, and human intervention. These factors result in both erosional and depositional processes, alter sediment budgets, and reshape coastal morphology. The ability to predict coastal morphological changes is essential for ensuring effective coastal zone management, the protection of infrastructure, and the sustainability of coastal eco-

systems (Vousdoukas *et al.* 2020; Masselink *et al.* 2016). Coastal researchers examine shoreline changes from multiple perspectives, but in recent decades, significant attention has been directed toward the evolution and prediction of the cross-shore profile. This is because cross-shore profile dynamics are highly responsive to natural drivers such as wave action, tides, sea level fluctuations, wind, and storm intensity, as well as anthropogenic influences including shore armoring, construction of groins, and dune degradation (Cowell *et al.* 2003; Nordstrom 2009; Jarmalavičius *et al.* 2012). Cross-shore profile analysis enables the

identification of erosion and accretion zones, facilitates risk assessment for infrastructure, and supports the planning of effective coastal protection measures (Masselink *et al.* 2014; Ruggiero *et al.* 2018).

Historically, investigations of the cross-shore profile have been based on in situ measurements (Jarmalavičius *et al.* 2020), empirical methods (Vellinga 1986; Dean 1991), and process-based physical models. Numerical simulation models such as SBeach (Wise *et al.* 1996) and Delft3D (Lesser *et al.* 2004) emerged, later followed by XBeach (Roelvink *et al.* 2009). These models enabled the simulation of wave dynamics, tidal processes, and sediment transport effects on shoreline morphology. Although they allow for high-precision calculations, they often require extensive calibration, large volumes of input data, and substantial computational resources, which limits their applicability in real-time forecasting and large-scale system analysis (McCall *et al.* 2010; Splinter *et al.* 2014).

In response to these challenges, data-driven approaches, particularly machine learning (ML) algorithms, have increasingly emerged over the past decade. Various ML models ranging from basic artificial neural networks (ANN) to more advanced Bayesian networks (BN), genetic algorithms (GA), regression trees (RT), and deep learning architectures have been applied to coastal morphodynamic studies. ANN models are among the most widely used due to their flexibility and ability to represent both linear and nonlinear dependencies. These models have successfully been employed to predict cross-shore profile elevation, wave characteristics, sediment dynamics, and even the influence of vegetation (Keijsers *et al.* 2015; López *et al.* 2017).

As the application of ML methods has evolved, long short-term memory (LSTM) networks have been introduced to efficiently process sequential data and forecast temporal morphological changes (Smagulova, James 2019). Lee *et al.* (2024) developed an LSTM encoder-decoder model capable of producing weekly predictions of cross-shore beach profiles based on historical wave and topographic profile data. Alternative approaches, such as Bayesian networks, have proven valuable as interpretable decision-support tools that not only provide predictions but also reveal the causal relationships among coastal system components (Beuzen 2019; Zarnetske *et al.* 2015). For instance, Plant and Stockdon (2012) developed a BN model to predict changes in dune crest elevation and position. This model was successfully applied by Palmsten *et al.* (2014), although attempts to use the model in new geographic areas without retraining the revealed limited generalization capabilities (den Heijer *et al.* 2012). This underscores a critical aspect of ML models: their ability to extrapolate beyond the

training data. Expanded BN models were further applied by Passeri *et al.* (2016) and Bilskie *et al.* (2016) to predict century-scale coastal changes under various climate and geological scenarios. Van Verseveld *et al.* (2015) combined BN models with results from XBeach simulations and highlighted the advantages of BN, including the integration of multiple input variables such as flooding, wave height, and erosion, and the ability to manage prediction uncertainty (Murray *et al.* 2016; Itzkin *et al.* 2022).

Other researchers have explored optimization techniques for tuning multiple interrelated model parameters. In such cases, genetic algorithms (Holland 1995) and genetic programming (Koza 1992) have been applied to simulate evolutionary processes that search for optimal model configurations (Goldstein *et al.* 2019). Although regression trees are conceptually simpler, they have been successfully used for classification tasks in coastal research. However, their application to continuous variables often requires additional stabilization procedures to avoid overfitting (De'ath, Fabricius 2000; Hastie *et al.* 2009).

Critically evaluating the development of the field reveals that ML methods have evolved from simple predictive models to more advanced hybrid and probabilistic frameworks capable of integrating heterogeneous data sources, representing complex nonlinear dependencies, and producing uncertainty-quantified predictions. Despite these advances, most applications remain geographically limited. ML models are typically developed for specific regions, and their transferability to new coastal environments remains a challenge. Overcoming this limitation is one of the primary directions in contemporary coastal modeling research.

The aim of this study is to assess the machine learning approach and the application of recurrent neural network models for coastal development prediction. The main goal is to develop a prototype predictive recurrent neural network model for cross-shore profile evolution prediction and to test its limitations. This research utilizes empirical measurements data to evaluate the accuracy, interpretability, and robustness of different ML algorithms. The study contributes to the development of advanced coastal forecasting tools that are adaptable to both local and regional coastal management contexts.

STUDY AREA

The Curonian Spit is a 98 km long sandy barrier, of which 51 km belong to Lithuania and the remaining 47 km to the Russian Federation (Fig. 1). Its widest point reaches 4 km, while the narrowest section is only 400 meters across. Owing to its exceptional and unique natural features, the Curonian Spit is included

in the UNESCO World Heritage List. The formation of the spit began during the Littorina Sea transgression period, and it reached its current length approximately 2000 years ago. The entire formation process of this sandy landform lasted about 3000 years.

The sea coast of the Curonian Spit is dominated by sandy beaches, with some sections partially covered by gravel and pebbles. Notable exceptions are observed in the southern segment, where moraine loam outcrops and buried soil layers are exposed along the shoreline (Gudelis 1998). The beach sediments primarily consist of fine to medium sand, with isolated patches of relict coarse sand (Jarmalavičius *et al.* 2017). Beach widths range from 10 to 86 meters. Narrower beaches, measuring between 10 and 20 meters, are typical in the southern part of the spit, where erosional processes prevail. In contrast, wider beaches ranging from 31 to 86 meters are more common in the northern part, where sediment accumulation dominates (Jarmalavičius *et al.* 2020). The eastern boundary of the beach is defined by a foredune ridge, with an average height of 5 to 6 meters and a maximum elevation of up to 16 meters.

The wind regime in the area is characterized by the predominance of westerly winds, which drive wave action from the west. The average significant wave height along the Curonian Spit is approximately 0.65 meters (Pupienis *et al.* 2017). The mean wind speed ranges between 5.0 and 5.5 meters per second, with the strongest winds recorded during autumn and winter storms reaching 28 to 40 meters per second (Galvonaitė *et al.* 2013; Jarmalavičius *et al.* 2016). Since the tidal range in the Baltic Sea does not exceed 4 centimetres, shoreline development is primarily influenced by fluctuations in water level, wave activity, and alongshore currents directed from south to north (Pupienis *et al.* 2017).

DATA AND METHODS

Data

To assess morphometric changes in the foredune, the coastal cross-shore levelling data set from the Curonian Spit was used. These profile cross-shore levelling measurements are taken yearly, usually in April or May, at 29 fixed points. Measurements are done by obtaining three-axis coordinates of the representative points along the measured profile using a GNSS/GPS device, going from a fixed point to the shoreline. This data is collected and managed as a part of coastal monitoring efforts by the Laboratory of Geoenvironmental Research at Lithuanian Nature Research Centre (Jarmalavičius *et al.* 2020). For the training, testing and validation of this model, a single cross-shore profile near Nida settlement was used (Fig. 1).

The data encompasses morphometric cross-shore profile changes from the 1995–2018 period (Fig. 2). Foredune height (h_1), beach height (h_2) and width (L) were determined yearly from cross-shore profiles (Fig. 3). The training of recurrent neural network models was based on year-to-year changes in the three morphometric properties that were assessed.

The hydrometeorological data were obtained from the Lithuanian Hydrometeorological Service under the Ministry of Environment and the Environmental Protection Agency. Wind, wave and sea level data from the Klaipėda automatic meteorological station and the Klaipėda Sea Port sea level measuring station were used to assess meteorological and hydrodynamic factors. The yearly mean, minimum, maximum and median values of wind speed and significant wave heights, as well as the average, minimum, maximum and amplitude of sea water level were taken. Wind direction data was included in an 8-rhumb system that represented the percentage of direction occurrence for each year.

A separate data set for the same hydrometeorological parameters was collected from reanalysis data. The ERA5 model data was used for yearly wind

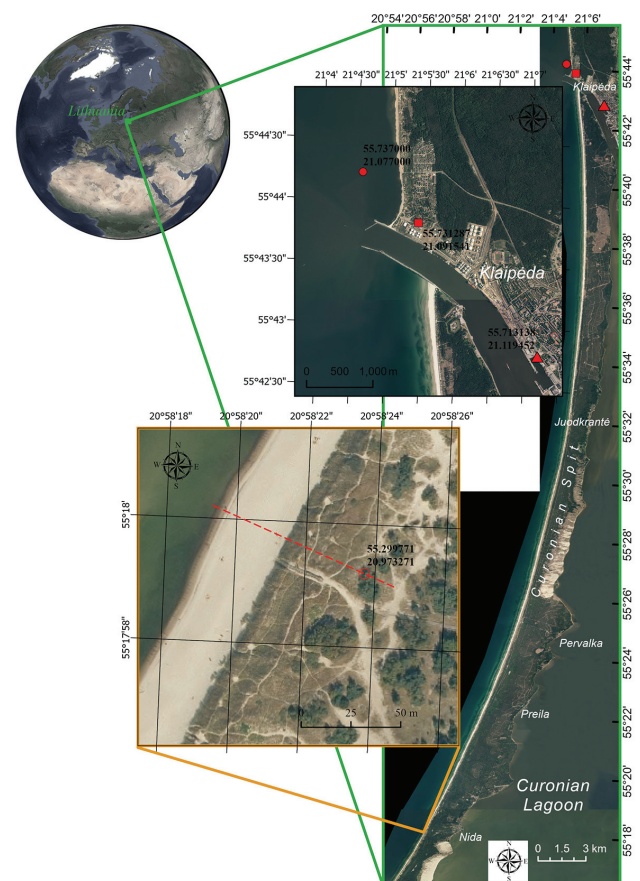


Fig. 1 Study area. Red line – cross-shore profile location. The red point marks the location where visual measurements of sea wave parameters are taken. The red triangle marks the location of the Klaipėda Sea Port marine water level measuring station. The red square marks the location of Klaipėda meteorological station

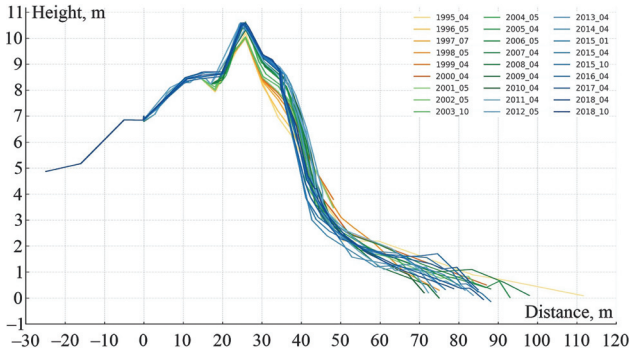


Fig. 2 Twenty-three measurements of cross-shore profile variability in the period 1995–2018 at the Nida settlement (the location of the measurements is shown in Fig. 1). Average sea level is represented by the 0 mark of the Y axis

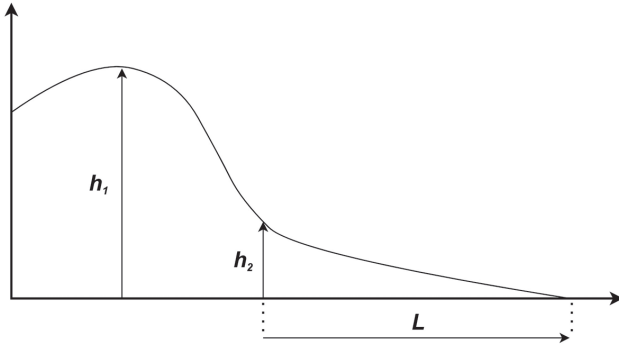


Fig. 3 A general cross-section of the shore profile and an assessment of the morphometric property parameters: h_1 – foredune height, h_2 – beach height, L – beach width

speed and direction, taken from a grid cell at 55.20, 20.72. Wave parameters were obtained from Baltic Sea Wave Hindcast data set that was produced using the WAM cycle 4.7 model and is openly shared on the Copernicus Marine Service platform. Sea level data was taken from the same platform, from the Baltic Sea Physics Reanalysis data set that is computed using model system Nemo. Wave and sea level parameters were taken from a grid cell at 55.29, 20.93.

Gated recurrent neural network models

To capture the patterns of foredune development in relation to meteorological conditions, two types of gated recurrent neural network models were used (Fig. 4): LSTM (*Long Short-Term Memory*) and a simplified variant – GRU (*Gated Recurrent Unit*). The main advantage of these models is the ability to solve the vanishing gradient problem for which time series prediction can be prone to (Van Houdt *et al.* 2020). The LSTM model achieves this by a series of input, forget and output gates which rely on sigmoid functions (1). By converting the input to values either close to 0 or to 1, relevant information is passed through the gate, and irrelevant information is ‘forgotten’ to avoid noise that could disrupt the predic-

tion. The function of these gates can be written as (Wen, Li. 2023):

$$g_t = \sigma(W_g[h_{t-1}, X_t] + b_g) \quad (1)$$

where σ stands for sigmoid function, W_g and b_g are gate specific weights, h_{t-1} is the hidden state from the previous time step, and X_t is a vector input from the current step. The g can indicate input (i), forget (f), or output (o) gates. After passing through input and forget gates, a candidate cell is formed using a hyperbolic tangent function (2); then an updated current cell state is formed (3), which is used to prepare the final output of the current cell to be used in another layer. This is also done using an output gate sigmoid function multiplied by a hyperbolic tangent of an updated current cell state (4).

$$L_t = \tanh(W_c[h_{t-1}, X_t] + b_c) \quad (2)$$

$$C_t = f_t \times C_{t-1} + i_t \times L_t \quad (3)$$

$$h_t = O_t \times \tanh(C_t) \quad (4)$$

The GRU model is a simplified alternative to the LSTM architecture, for which a single update gate is used instead of the input and forget gates. By utilizing a structure consisting of update and reset gates and a candidate memory content, GRU provides a more efficient approach to capture long-term sequence dependencies (Dey, Salem 2017). The update (5) and reset (6) gate functions are also based on similar sigmoid functions and can be expressed as follows (Shiri *et al.* 2024):

$$z_t = \sigma(W_z[h_{t-1}, x_t] + b_z) \quad (5)$$

$$r_t = \sigma(W_r[h_{t-1}, x_t] + b_r) \quad (6)$$

Similarly as in the LSTM model, hyperbolic tangent is also used in GRU to prepare output candidate (7) and actual cell output (8) for the next time step.

$$\tilde{h}_t = \tanh(W_h[r_t h_{t-1}, x_t]) \quad (7)$$

$$h_t = (1 - z_t)h_{t-1} + z_t \tilde{h}_t \quad (8)$$

Model development

The above mentioned machine modelling algorithms were used to develop two models, one for each algorithm, in the form of python script. Data preprocessing (normalizing, scaling and splitting) was done using the *sklearn* package. Models are based on the *tensorflow* package, which was used to set the model structure. Both models utilize the same neural network model structure that consists of two main hidden layers. The LSTM/GRU algorithms are used in the first layer consisting of 24 neurons. Signal is then

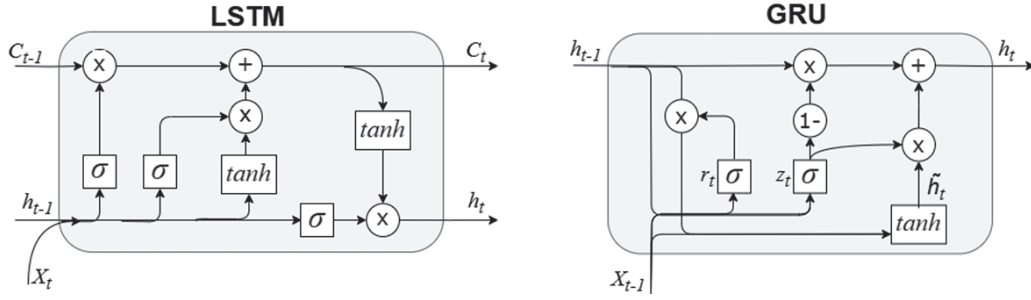


Fig. 4 Cell structures of LSTM (Long Short-Term Memory) and GRU (Gated Recurrent Unit) models

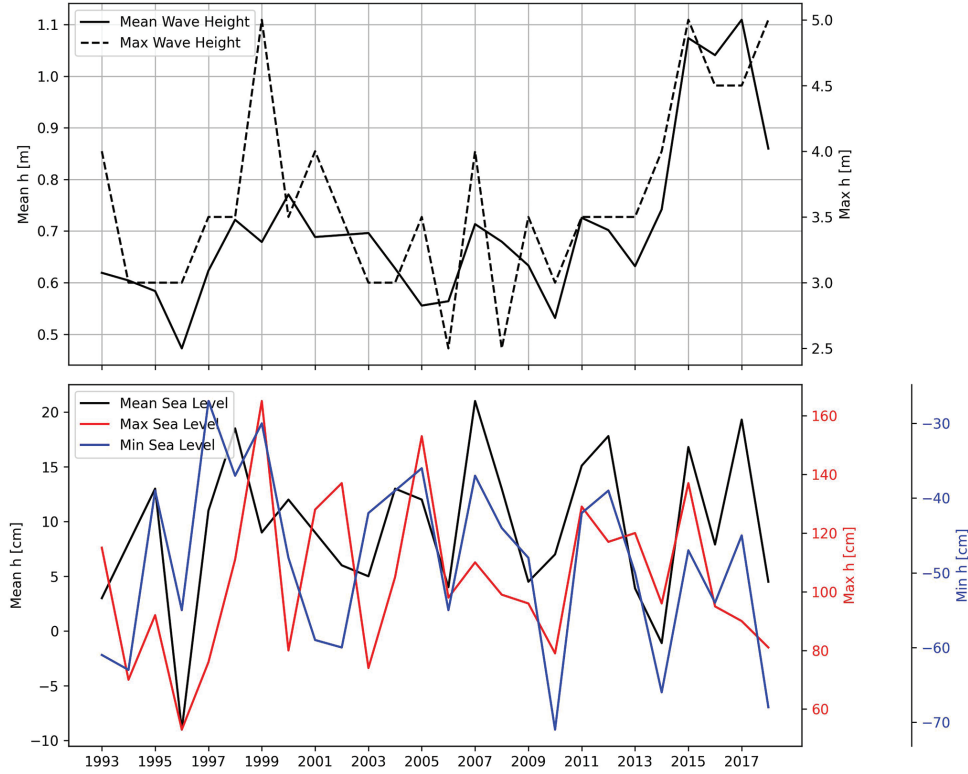


Fig. 5 Changes in maximum and mean wave height at the top; maximum, mean and minimum sea level from 1991 to 2018 at the bottom, measured at Klaipėda observation stations

passed into a dense layer made of 16 neurons. The final output layer is made of a single neuron that outputs a predicted value.

The model is set up to be trained and assessed for each morphometric parameter (Δh_p , Δh_s , ΔL) separately. Given a relatively short timeline, a conservative approach was taken to use as much of the data as possible for model training to achieve more accurate results. The model was trained using 90% (1995–2015) of the data, and the remaining 10% (2016–2018) were used for model testing. The performance of the model was evaluated by monitoring the training and validation error changes across the training epochs, which is expressed as the change of the mean squared error (*MSE*). Model results were evaluated from three test year (2016–2018) values. Observation values were compared to the predicted values, from which the mean absolute error (*MAE*) representing model accuracy was derived.

RESULTS

Hydrodynamic and wind parameters

A moderate variability (standard deviation $SD = 0.15$) of the mean wave height was observed during the study period (Fig. 5). The average wave height was 0.70 m. Maximum yearly values appear to be fluctuating more ($SD = 0.70$) displaying several peaks when wave heights exceeded 4 m. Wave heights reached the 5 m mark in 1999, 2015, and 2018. The peaks coincide with severe storms Anatol (1999) and Felix (2015), which were observed during the study period. Although a severe storm Erwin was also observed during 2005, it is not represented in the wave heights.

A similar pattern can be seen in the fluctuation of yearly sea level parameters (Fig. 5). The mean sea level seems to be almost constant without any significant peaks ($SD = 6.5$). Maximum sea level displays

several peaks matching the wave height pattern. Sea level exceeded the 150 cm mark in 1999 and 2005, which are the years of storms Anatol and Erwin. During 12 of the 28 observed years, sea level reached 100 cm, which is considered a threshold at which the coast starts to experience erosion. The amplitude of sea level for the given period was 148 cm, which did not appear to fluctuate significantly ($SD = 24.4$).

Wind speed values showed the highest peaks of maximum wind speed during years 1993 and 1999, which also coincide with the observed severe storms (Fig. 5). The highest wind speed was observed for the year 1999, reaching 38 m/s. After this, the maximum values did not exceed 35 m/s and appear to be following a negative trend, although the significance was not assessed. The overall maximum wind speed values had a high variability of $SD = 4.20$. During the study period, the average wind speed was 4 m/s with a moderate variability ($SD = 0.72$). Figure 6 shows that a period between 1997 and 2004 had noticeably

higher wind speeds. After the year 2009 until the end of the study period, it was lower than average.

Wind direction appears to have a turning point in the middle of the study period (Fig. 7). Although westerly winds continued to prevail, southerly and southeasterly directions were becoming more common. Southeasterly winds showed significant dominance in the years 2006 (22%), 2010 (20%), 2012 (21%), and 2014 (24%). Westerly winds exhibited significant peaks in the years 2008 (23%), 2011 (23%), and 2015 (22%) during the second half of the study period. In the first half, wind direction appeared to be less variable, with a nearly constant dominance of westerly winds.

It also appears that the period of southeasterly dominance corresponds to a period of lower wind speeds. However, wave heights do not seem to be directly related to westerly winds, but rather to wind speed. At the same time, sea level seems to be related to wind direction, as indicated by lower water levels during years when southeasterly winds prevail.



Fig. 6 Yearly maximum and average wind speed (m/s)

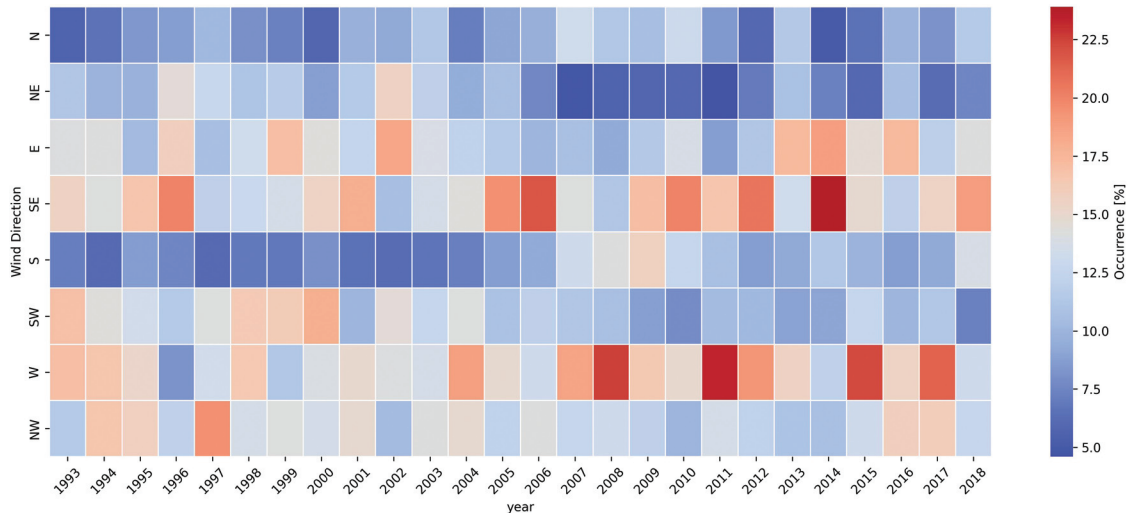


Fig. 7 Heat map of wind direction occurrence (%) during 1991–2018 period

Morphometry

The cross-shore profiling data (Fig. 2) reveals yearly morphodynamical tendencies. Constant shoreline retreat is observed at the beach of Nida. On average, the shoreline moves 1.07 m inland every year. Having almost constant negative change, beach width is the most dynamic morphometric parameter of this coastal system, having standard deviation (*SD*) of 10.06 m. Foredune height and beach height are much less dynamic. It only changes 0.01–0.03 m a year, the changes being positive mostly.

Severe erosion was observed during the years 1996 and 1998 when shoreline retreated more than 10 m and in 2009 when it retreated even more than 22 m. These years stand out as having higher storm intensity. Shoreline moved more than 10 m seaward through the years 2006 and 2013.

Foredune height

Both LSTM and GRU models show similar results in model training performance (Fig. 8). The training stops at the point when training loss is around 0.05 *MSE*. The validation curve shows a similar rate of decreasing *MSE* during the training process. Slight increases in the second half of the progress seem to be giving hints of overfitting; however, this is addressed by introducing drop-out layers that drop random neurons in every epoch.

This affects the training error curve which shows a decreasing but rather unsteady change of *MSE*. Slightly more promising results are shown by the validation curve of GRU model which appears to make progress at the beginning. This model also took almost twice as less epochs to train (120) as the LSTM model did (250).

The overall training progress shows a noticeable gap between validation and training curves. This shows that both models are unable to capture and generalize patterns in the used data. It might mean that the time series are too short or lack significant variation.

Prediction test results are also quite similar for LSTM (*MAE* = 0.70) and GRU (*MAE* = 0.78) models. Given that the standard deviation of foredune height from the study period is *SD* = 0.57, it seems that prediction is not in tolerable limits. The test also shows that both models are slightly biased to positive changes of foredune height. Although it accurately represents the tendency of the last two test years, for the first year the change was significantly underestimated.

Although prediction results appear to be quite accurate, both models are estimating values close to zero. This could be a sign that the models were unable to effectively generalize data in the training process and are either biased towards mean values or simply use small values as a “safe bet”. This may also be related to limited variability in the training data. However, by nature the height of the foredune is not the most dynamic morphometric parameter, given its

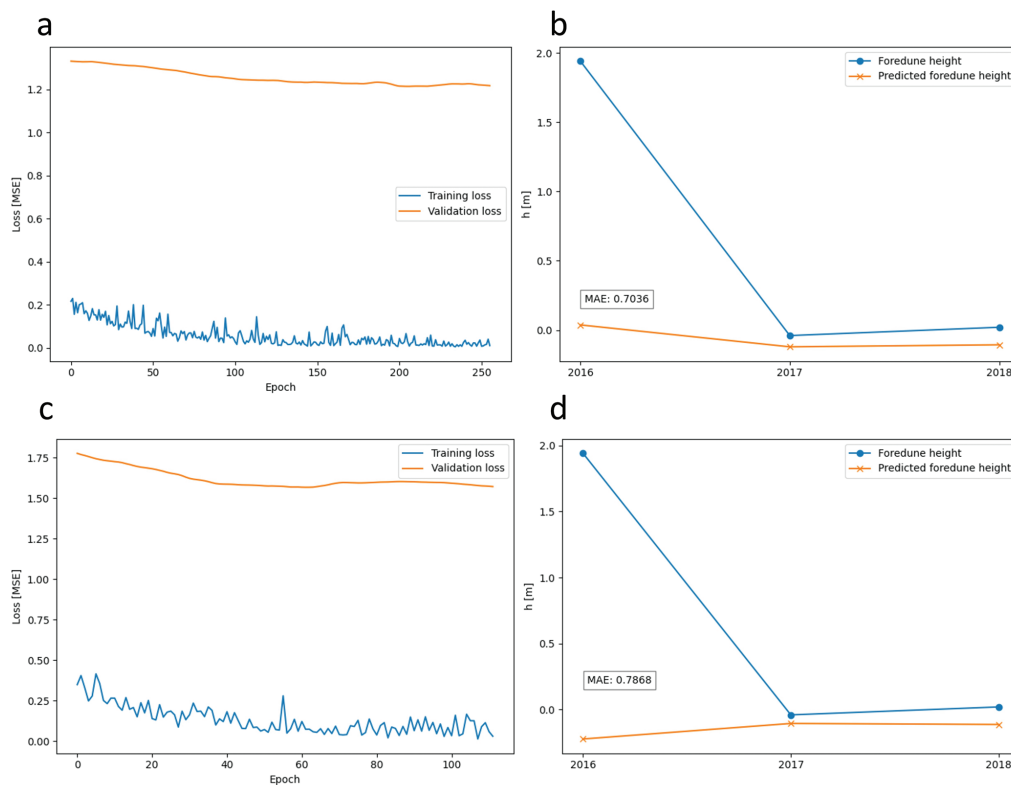


Fig. 8 LSTM (a; b) and GRU (c; d) models for foredune height prediction. Training performance (a; c) and foredune height prediction accuracy testing across three different years (b; d)

scale ($h_l^- = 9.83$ m) and variability ($SD = 0.57$), therefore making changes hard to predict using past data.

Models were also trained and tested on wind, wave and sea level reanalyses. Results appear similar, showing only slight differences from training on empirical data (Fig. 9). Tests show the same accuracy for both algorithms ($MAE = 0.70$). This is a little more accurate in case of the GRU model (Fig. 8d; Fig. 9d), although the difference does not appear to be significant. Models were also mostly inaccurate for the first testing year, showing better results for the last two years (Fig. 9b, d). However, the validation error appears more stable during LSTM training, which may indicate that overfitting is even more pronounced.

Beach width

The learning curves of both models appear to be gradually decreasing when being trained for beach width ($SD = 10.06$) prediction (Fig. 10). The progress of LSTM model training shows that there is a gap of MSE between training and validation curves at the time when training stops (~ 275 epoch), in comparison to the cross paths in the training progress of the GRU model which took around 250 epochs to train. Validation starts to climb at around 200th epoch in both models. This may be a hint of overfitting, although it is only present at the very end of the training progress and could be easily solved by stopping the model earlier.

The LSTM model test results gave out a slightly smaller error ($MAE = 5.79$), meaning that its predic-

tions are closer to the real values than GRU model predictions are ($MAE = 6.00$). At the same time, the predictions by the LSTM model accurately captured negative and positive changes for all three test years, whereas GRU misinterpreted beach width change for the first test year.

The models appear to be able to capture the mode of change (erosion and accretion) accurately. However, the values of predicted beach width changes appear to be quite modest in comparison to the real values. Again, these models are estimating values closer to zero, underestimating shoreline changes.

Predictions for beach width are slightly more accurate with both LSTM ($MAE = 5.30$) and GRU ($MAE = 5.43$) models that are trained on reanalysis data (Fig. 11). Both algorithms were also able to capture erosion and accretion, although significantly overestimating predicted changes. However, the training progress is not as pronounced as the training with empirical data. Models based on reanalysis data also required twice as many epochs to train. An increase in validation error can be observed toward the end of training, which may indicate that the models are overfitting.

Beach height

LSTM and GRU models showed different progress throughout the training. The validation curve for the LSTM model (Fig. 12a) remains low without almost any change through the course. Training stops after

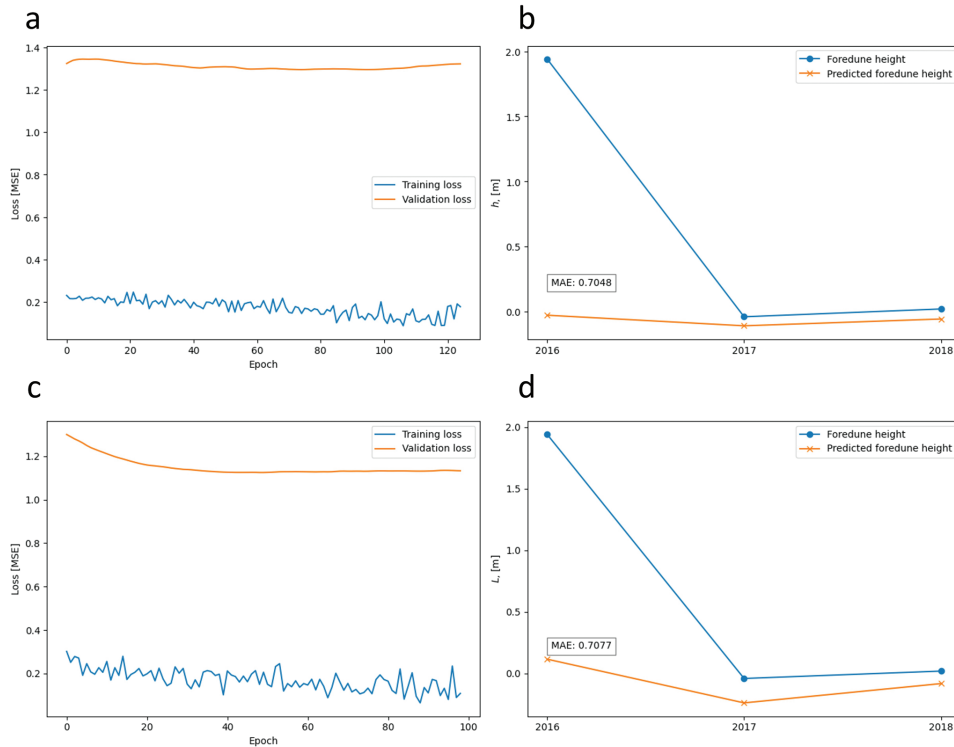


Fig. 9 LSTM (a; b) and GRU (c; d) models for foredune height prediction trained with reanalysis data. Training performance (a; c) and foredune height prediction accuracy testing across three different years (b; d)

70 epochs. This short and steady learning process shows a potentially positive result. At the same time, it could be related to a less variable parameter it is trying to generalize.

The testing results of the LSTM model display highly accurate predictions for the first two test years

(Fig. 12b). The overall accuracy of the LSTM model is represented by $MAE = 0.07$, which is reasonable and could be seen as accurate for a less variable beach height ($SD = 0.72$) with an average value of $\bar{h}_2 = 2.52$ m. However, the model shows inconsistent errors underestimating changes for the first and overestimating

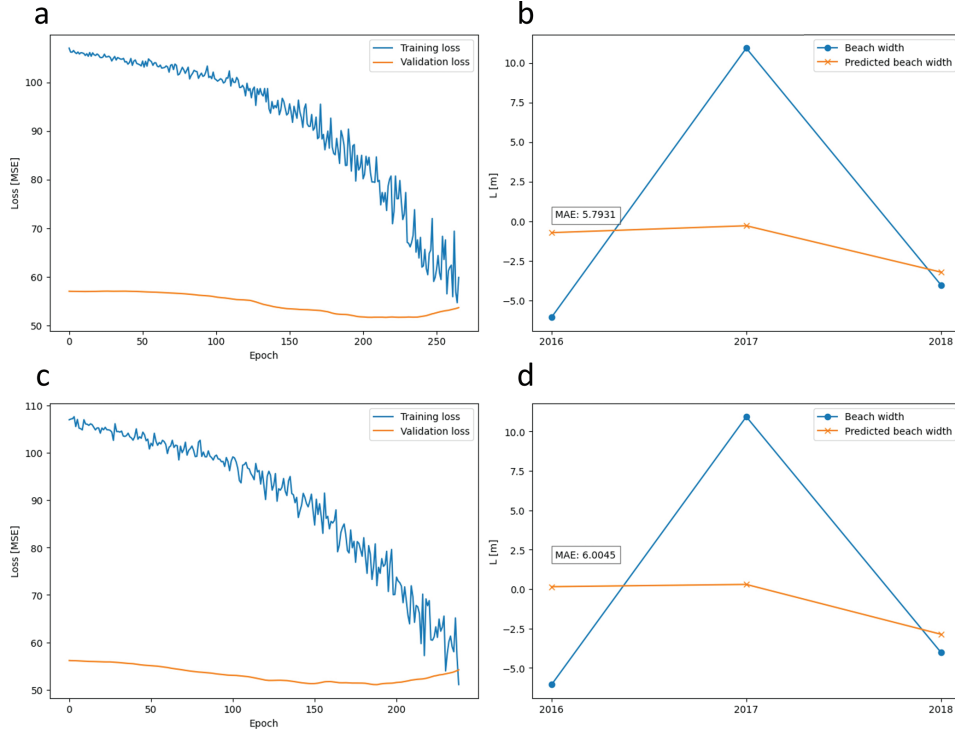


Fig. 10 LSTM (a; b) and GRU (c; d) models for beach width prediction. Training performance (a; c) and beach width prediction accuracy testing across three different years (b; d)

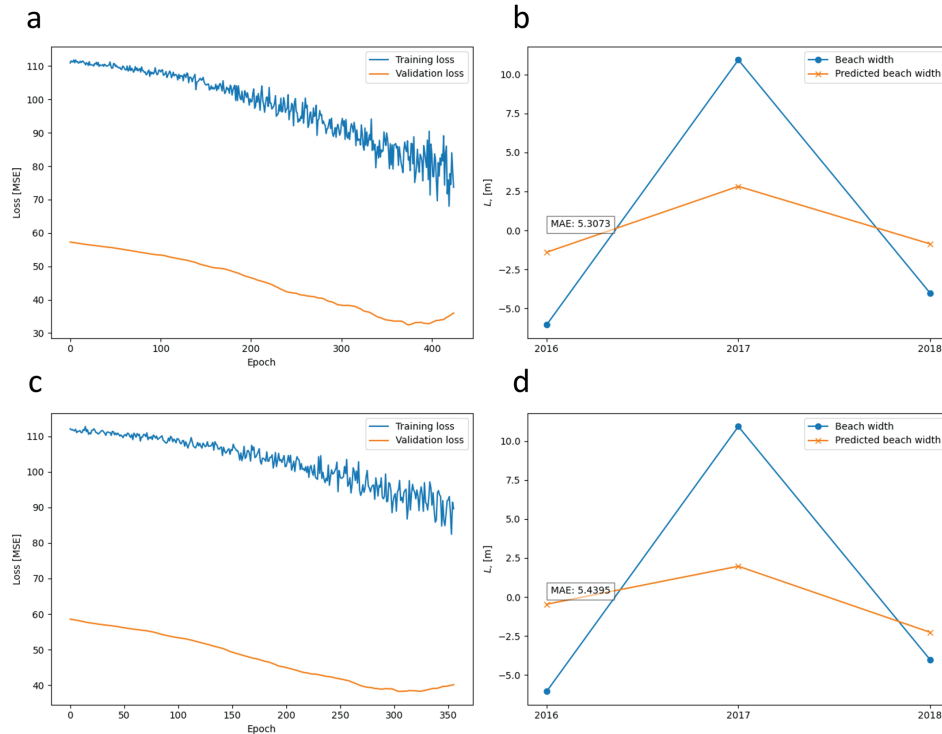


Fig. 11 LSTM (a; b) and GRU (c; d) models for beach width prediction trained with reanalysis data. Training performance (a; c) and beach width prediction accuracy testing across three different years (b; d)

for the last test year and also predicting negative instead of positive changes for the second year.

It took longer for the GRU model to train also displaying a more pronounced increase of the validation error towards the end of training (Fig. 12c). The test results exhibit a slightly higher accuracy

($MAE = 0.04$) compared to the LSTM model. In relation to the standard deviation of beach height, the model appears to be quite accurate. The model was able to accurately predict the increase of accretion throughout the test years when only underestimating the magnitude.

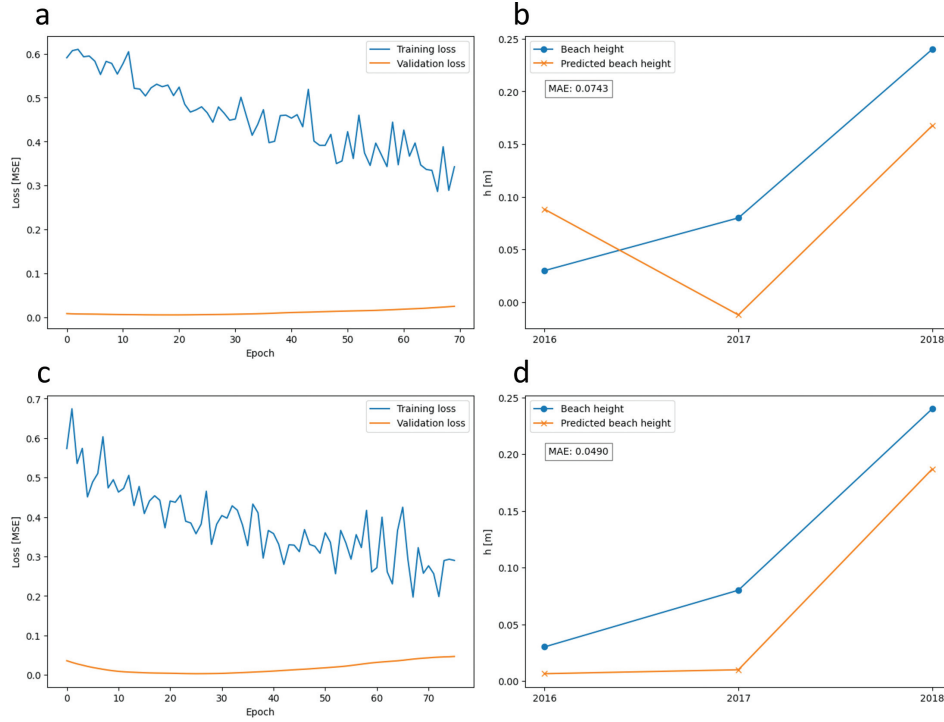


Fig. 12 LSTM (a; b) and GRU (c; d) models for beach height prediction. Training performance (a; c) and beach height prediction accuracy testing across three different years (b; d)

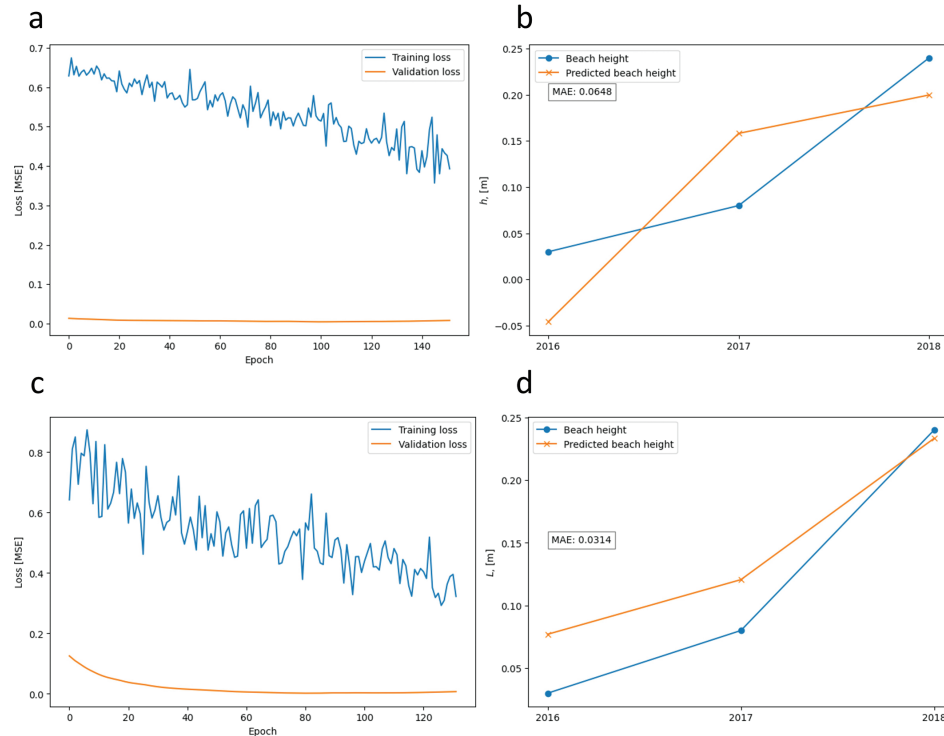


Fig. 13 LSTM (a; b) and GRU (c; d) models for beach height prediction trained with reanalysis data. Training performance (a; c) and beach height prediction accuracy testing across three different years (b; d)

The prediction of beach height appears to be more accurate by the models trained on reanalysis data (Fig. 13), although the LSTM model does not seem accurate in capturing the magnitude of changes across the test years. Progress is not entirely evident during the training, showing that the model is struggling to generalize relationship patterns between the predictive parameters. Unlike the LSTM, the GRU model trained on reanalysis data showed relatively accurate results ($MAE = 0.03$), outperforming the models trained on empirical data. Generalization progress can be seen as the validation error drops in the first half of the training period after which it becomes stable (Fig. 13c). Testing results show that it is able to generalize relationship patterns and return accurate prediction, capturing the direction of change.

Judging by the errors it appears that both models display promising results. The GRU model shows an advantage in its capabilities to predict the type of morphometric changes more accurately and in being able to capture the tendency of change correctly.

DISCUSSION

The cross-shore profile data gathered near Nida was used together with meteorological, wave and sea level data from Klaipėda (Fig. 1). This means that hydrometeorological conditions applied on the Nida cross-shore profile might not accurately represent the situation at the actual cross-sectioning location. Changing wind patterns in the Baltic region recently described by Soomere *et al.* (2024) display varying tendencies along the Baltic Sea southeastern coast. It suggests that waves and sea level changes can have a significant spatial variance along the southeastern Baltic coast, meaning it could act differently upon the shore in different sections. Changes of these parameters are often tied to increasing cyclonic activity in the Baltic (Meier *et al.* 2022), although no noticeable positive trends can be seen in the yearly wind speed, sea level or wave height data.

However, the practical implementation of such model for different coastal sections could not be possible without such inaccuracies simply due to limited measuring points. Model data can be implemented to solve this issue, although it has its own limitations (Soomere 2023). While providing necessary parameters at the exact location of interest, it usually ignores the majority of the local factors that could have a significant localized effect. Consequently, its advantage for this application is reduced as the averaging within each grid cell smooths out important parameter details needed for model training. Moreover, the modelled wave and sea level data is directly tied to wind models used to simulate hydrodynamics. This implies that the modelled hydrodynamic parameters are only reflecting the modelled wind speed and di-

rection while ignoring other local factors. Our tests with models trained on empirical and modelled, more spatially accurate data showed only minor differences between these two approaches.

On the other hand, wind could be seen as the main driver of coastal development since it is also responsible for other relevant factors – sea level and wave regime. Therefore, one could say that wind data is enough to train such model. Though evidently, hydrodynamic factors appear to have a different effect under different nearshore and beach morphometric conditions also affecting one another (Janušaitė *et al.* 2023). This makes this task even more complicated since the influence of the factors is also changing in accordance with the evolution of the coast (Brazdžiūnas *et al.* 2024). For instance, prediction results may be disrupted if the profile changes drastically e.g. after a severe storm. Even though recurrent neural networks can deal with irregular data (Weekarody *et al.* 2021), it would make accurate predictions nearly impossible if the model is trained on a profile prior to when the severe damage was done, since waves and sea level would be acting in a different way. This suggests that for coastal evolution prediction morphometric parameters are of the same level of importance as the ones affecting them. At the same time, nearshore bathymetry is also worth noting since it is an important part of the coastal geomorphology system, being a key factor affecting wave propagation and alongshore sediment transport (Jakimavičius *et al.* 2018). This highlights the importance to include the whole coastal system in geomorphology assessments without excluding any parts since they are dependent on one another. Perhaps it is even impossible to predict coastal development without taking nearshore bathymetry into account at all. Various passive factors, like sediment granulometry (Jarmalavičius *et al.* 2017) or vegetation could also play a key role, rendering a unique effect of dynamic factors at different locations (Keijsers *et al.* 2015; López *et al.* 2017), hence it might be also important to include those as well.

At the same time, including too many variables may overwhelm the model and add up to the overfitting issue (Bejani, Ghatee 2021). The influence of most of those factors may already be represented by the interplay between wind, waves and sea level that are already considered, so there might be no need to include them as separate. This could be evaluated by assessing correlation among them (Fig. 11). The importance of the factors affecting coastal development may also vary in space (Keijsers *et al.* 2014). To implement such model in different coastal stretches, a separate evaluation of shaping factors could be performed to assess their significance and point out the ones to be included.

It is also worth noting that yearly values of meteorological and hydrodynamic values may fail to

Average Wave Height (m)	1.00	0.19	0.62	0.24	0.73	0.57	0.17	-0.14	-0.30	-0.52	-0.50	-0.44	-0.18	0.65	0.76	0.40	-0.12
Maximum Wave Height (m)	0.19	1.00	-0.12	0.76	0.22	0.41	0.66	0.51	0.11	-0.03	0.06	-0.07	0.14	-0.14	0.01	0.02	-0.11
Mean Wind Speed (m/s)	0.62	-0.12	1.00	-0.02	0.45	0.26	-0.04	-0.19	-0.05	-0.39	-0.29	-0.40	0.12	0.55	0.48	0.12	-0.20
Maximum Wind Speed (m/s)	0.24	0.76	-0.02	1.00	0.22	0.47	0.74	0.49	-0.17	0.04	-0.02	-0.13	-0.09	0.01	0.15	0.09	0.25
Mean Sea Level (m)	0.73	0.22	0.45	0.22	1.00	0.67	0.35	0.04	-0.14	-0.60	-0.65	-0.38	-0.12	0.49	0.82	0.35	0.04
Minimum Sea Level (cm)	0.57	0.41	0.26	0.47	0.67	1.00	0.46	-0.00	-0.05	-0.29	-0.59	-0.43	-0.09	0.33	0.55	0.52	0.25
Maximum Sea Level (cm)	0.17	0.66	-0.04	0.74	0.35	0.46	1.00	0.86	-0.02	0.10	-0.08	-0.27	-0.10	0.03	0.32	-0.01	0.00
Sea Level Amplitude (cm)	-0.14	0.51	-0.19	0.49	0.04	-0.00	0.86	1.00	0.15	0.35	0.27	-0.17	-0.08	-0.17	0.03	-0.29	-0.26
North (%)	-0.30	0.11	-0.05	-0.17	-0.14	-0.05	-0.02	0.15	1.00	0.40	0.15	-0.35	0.07	-0.51	-0.25	0.02	-0.50
Northeast (%)	-0.52	-0.03	-0.39	0.04	-0.60	-0.29	0.10	0.35	0.40	1.00	0.67	-0.17	-0.28	-0.38	-0.57	-0.32	-0.17
East (%)	-0.50	0.06	-0.29	-0.02	-0.65	-0.59	-0.08	0.27	0.15	0.67	1.00	0.04	0.03	-0.16	-0.68	-0.67	-0.34
Southeast (%)	-0.44	-0.07	-0.40	-0.13	-0.38	-0.43	-0.27	-0.17	-0.35	-0.17	0.04	1.00	0.19	-0.43	-0.49	-0.27	0.43
South (%)	-0.18	0.14	0.12	-0.09	-0.12	-0.09	-0.10	-0.08	0.07	-0.28	0.03	0.19	1.00	-0.17	-0.17	-0.33	0.01
Southwest (%)	0.65	-0.14	0.55	0.01	0.49	0.33	0.03	-0.17	-0.51	-0.38	-0.16	-0.43	-0.17	1.00	0.54	0.09	-0.03
West (%)	0.76	0.01	0.48	0.15	0.82	0.55	0.32	0.03	-0.25	-0.57	-0.68	-0.49	-0.17	0.54	1.00	0.39	-0.03
Northwest (%)	0.40	0.02	0.12	0.09	0.35	0.52	-0.01	-0.29	0.02	-0.32	-0.67	-0.27	-0.33	0.09	0.39	1.00	0.12
Calm (%)	-0.12	-0.11	-0.20	0.25	0.04	0.25	0.00	-0.26	-0.50	-0.17	-0.34	0.43	0.01	-0.03	-0.03	0.12	1.00
	Average Wave Height (m)	Maximum Wave Height (m)	Mean Wind Speed (m/s)	Maximum Wind Speed (m/s)	Mean Sea Level (m)	Minimum Sea Level (cm)	Maximum Sea Level (cm)	Sea Level Amplitude (cm)	North (%)	Northeast (%)	East (%)	Southeast (%)	South (%)	Southwest (%)	West (%)	Northwest (%)	Calm (%)

Fig. 14 Correlation matrix for the changes of wave (average, maximum), wind speed (mean, peak), sea level (mean, minimum, maximum, amplitude) and wind direction occurrence percentage (north, northeast, east, southeast, south, southwest, west, northwest, calm) variables

represent short temporal nuances critical to coastal development, and perhaps monthly or even daily data should be used. At the same time, important events like severe storms appear to be represented by maximum values and amplitude (Figs 5; 6). However, the mean values seem to have low variability and could potentially be removed since they might not be carrying any relevant information. They might also be the reason why the model is biased to average values.

It is hard to tell which model performs better for this task. Both LSTM and GRU models appear to be hardly able to deal with such a short time series. It can be seen by the training progress which is showing the hints of overfitting meaning that it is hard to generalize the data set. A slightly better accuracy was achieved by the LSTM model which may suggest that a series of gates are acting in favour and perhaps this is the forget gate mechanism that allows a better generalization. This could be tested by introducing a simple non-gated RNN model.

It might also be worth to assess the time span for which certain conditions may have an effect. Understanding how the coastal system interacts could be vital for creating an accurate sequential predictive model. At this point it is still hard to tell the length of the condition sequence that is needed for accurate prediction, so the yearly changes are being used. It has been previously noted that the duration of certain conditions may also play a key role (Jarmalavičius *et al.* 2016). Perhaps hourly data could be utilized to take duration into account. This might open new possibilities of using temporal data on a smaller time scale that would allow us to assess the influence of storms and other significant events.

Capturing these nuances may not be possible with other simpler autoregressive models; therefore, a machine learning approach has a great advantage. At the same time, only natural factors are considered while anthropogenic activities may also have a variety of effects, some of which are still hard to assess and predict (Jarmalavičius *et al.* 2020).

CONCLUSIONS

The results achieved by testing both models and with different data sets suggest that recurrent neural network models could potentially be applied for coastal morphometry forecasting once data limitations are solved. It is hard to say which model performed better since the errors are quite similar. However, LSTM seems to be able to capture negative and positive changes more accurately. It can potentially be used to predict future tendencies of coastal development.

A comparison between models trained on empirical and model data did not reveal any significant difference, although prediction was slightly more accurate. It appears that although model data provides input parameters from the exact location, it has its own limitations that counteract its potential advantages. Majority of location specific parameters are not considered, and values are averaged over the entire grid cell, limiting precision to the spatial resolution.

Predictions of beach width and height seem to be the most accurate, though at the same time it is the beach that is the most dynamic morphometric property of the coastal system. This may indicate that the data set used for model training, especially for foredune height, may be lacking diversity. This could also be seen from the hints of overfitting that are noticeable in the training progress. This means that the model is not able to generalize the patterns but rather starts to learn the data set itself. It can be concluded that a more diverse data set is needed to train a reliable model. Prediction accuracy could also benefit from a longer time series which could potentially increase model ability to generalize long-term patterns.

To implement such model in practical use, it would still require adjustments and further development. The current version is still unable to capture the relationships between different morphometric parameters which could also play an important part. Perhaps more different models could be tested to find an optimal choice.

ACKNOWLEDGEMENTS

This research was financed by the Research Council of Lithuania (Grant No. P-PAD-24-24). The authors would like to thank two anonymous reviewers for their valuable comments on the article.

REFERENCES

Bejani, M.M., Ghatee, M. 2021. A systematic review on overfitting control in shallow and deep neural networks. *Artificial Intelligence Review* 54(8), 6391–6438. <https://doi.org/10.1007/s10462-021-09975-1>

Beuzen, T. 2019. pybeach: A Python package for extract-

ing the location of dune toes on beach profile transects. *Journal of Open Source Software* 4(44), 1890. <https://doi.org/10.21105/joss.01890>

Bilskie, M.V., Passeri, D.L., Hagen, S.C., Medeiros, S.C., Alizad, K., Wang, D. 2016. Dynamic simulation and numerical analysis of hurricane storm surge under sea level rise with geomorphologic changes along the northern Gulf of Mexico. *Earth's Future* 4(10), 177–193. <https://doi.org/10.1002/2015EF000347>

Brazdžiūnas, P., Pupienis, D., Jarmalavičius, D., Žilinskas, G. 2024. Space-Time Tendencies of Coastal Dynamics based on Morphometric and Hydro-Meteorological Data (Curonian Spit, Lithuania). *Journal of Coastal Research* 113(SI), 300–304. <https://doi.org/10.2112/JCR-SI113-059.1>

Cowell, P.J., Stive, M.J.F., Niedoroda, A.W., De Vriend, H.J., Swift, D.J.P., Kuriyama, Y., Nicholson, J., Roy, P.S., Thom, B.G. 2003. The coastal-tract (part 1): a conceptual approach to aggregated modeling of low-order coastal change. *Journal of Coastal Research* 19(4), 812–827.

De'ath, G., Fabricius, K.E. 2000. Classification and regression trees: a powerful yet simple technique for ecological data analysis. *Ecology* 81(11), 3178–3192. [https://doi.org/10.1890/0012-9658\(2000\)081\[3178:CA RTAP\]2.0.CO;2](https://doi.org/10.1890/0012-9658(2000)081[3178:CA RTAP]2.0.CO;2)

Dean, R.G. 1991. Equilibrium beach profiles: Characteristics and applications. *Journal of Coastal Research* 7(1), 53–84.

Dey, R., Salem, F.M. 2017. Gate-variants of gated recurrent unit (GRU) neural networks. In: *2017 IEEE 60th international midwest symposium on circuits and systems (MWSCAS)*, 1597–1600. <https://doi.org/10.1109/MWSCAS.2017.8053243>

den Heijer, C.K., Knipping, D.T., Plant, N.G., de Vries, J.S.V.T., Baart, F., van Gelder, P.H. 2012. Impact assessment of extreme storm events using a Bayesian network. *Coastal Engineering Proceedings* 1(33), 4. <https://doi.org/10.9753/icce.v33.management.4>

Galvonaitė, A., Kilpys, J., Kitrienė, Z., Valiukas, D. 2013. *Mean Climatic Indicators in Lithuania for the Period 1981–2010*. Climatology Division, Lithuanian Hydrometeorological Service under the Ministry of Environment, 24 pp.

Goldstein, E.B., Coco, G., Plant, N.G. 2019. A review of machine learning applications to coastal sediment transport and morphodynamics. *Earth-Science Reviews* 194, 97–108. <https://doi.org/10.1016/j.earscirev.2019.04.022>

Gudelis, V. 1998. *The Lithuanian Maritime Zone and Coastal Area*. Lithuanian Academy of Sciences, 442 pp.

Hastie, T., Tibshirani, R., Friedman, J.H. 2009. *The elements of statistical learning: data mining, inference, and prediction* (Vol. 2). New York: Springer, 745 pp. <https://doi.org/10.1007/978-0-387-84858-7>

Holland, J.H. 1992. *Adaptation in Natural and Artificial Systems: An Introductory Analysis with Applications to Biology, Control, and Artificial Intelligence*.

- Ann Arbor: University of Michigan Press, 211pp. <https://doi.org/10.7551/mitpress/1090.001.0001>
- Itzkin, M., Moore, L.J., Ruggiero, P., Hovenga, P.A., Hacker, S.D. 2022. Combining process-based and data-driven approaches to forecast beach and dune change. *Environmental Modelling & Software* 153, 105404. <https://doi.org/10.1016/j.envsoft.2022.105404>
- Jakimavičius, D., Kriaučiūnienė, J., Šarauskienė, D. 2018. Assessment of wave climate and energy resources in the Baltic Sea nearshore (Lithuanian territorial water). *Oceanologia* 60(2), 207–218. <https://doi.org/10.1016/j.oceano.2017.10.004>
- Janušaitė, R., Jarmalavičius, D., Pupienis, D., Žilinskas, G., Jukna, L. 2023. Nearshore sandbar switching episodes and their relationship with coastal erosion at the Curonian Spit, Baltic Sea. *Oceanologia* 65(1), 71–85. <https://doi.org/10.1016/j.oceano.2021.11.004>
- Jarmalavičius, D., Satkūnas, J., Žilinskas, G., Pupienis, D. 2012. The influence of coastal morphology on wind velocity dynamics. *Estonian Journal of Earth Sciences* 61(2), 120–130. <https://doi.org/10.3176/earth.2012.2.04>
- Jarmalavičius, D., Šmatas, V., Stankūnavičius, G., Pupienis, D., Žilinskas, G. 2016. Factors controlling coastal erosion during storm events. *Journal of Coastal Research* 75(SI), 1112–1116. <https://doi.org/10.2112/SI75-223.1>
- Jarmalavičius, D., Žilinskas, G., Pupienis, D. 2017. Geologic framework as a factor controlling coastal morphometry and dynamics. Curonian Spit, Lithuania. *International Journal of Sediment Research* 32(4), 597–603. <https://doi.org/10.1016/j.ijsrc.2017.07.006>
- Jarmalavičius, D., Pupienis, D., Žilinskas, G., Janušaitė, R., Karaliūnas, V. 2020. Beach-fore-dune sediment budget response to sea level fluctuation: Curonian Spit, Lithuania. *Water* 12(2), 583. <https://doi.org/10.3390/w12020583>
- Jarmalavičius, D., Žilinskas, G., Pupienis, D., Karaliūnas, V., Janušaitė, R. 2020. Natural and Human Control of the Coastal Development. Baltic Sea, Lithuania. *Geografijos metraštis* 53, 3–12. [In Lithuanian]. <https://doi.org/10.5200/GM.2020.1>
- Keijsers, J.G., Poortinga, A., Riksen, M.J., Maroulis, J. 2014. Spatio-temporal variability in accretion and erosion of coastal foredunes in the Netherlands: regional climate and local topography. *PloS one* 9(3), e91115. <https://doi.org/10.1371/journal.pone.0091115>
- Keijsers, J.G.S., de Groot, A.V., Riksen, M.J.P.M. 2015. Vegetation and sedimentation on coastal foredunes. *Geomorphology* 228, 723–734. <https://doi.org/10.1016/j.geomorph.2014.10.027>
- Koza, J.R. 1994. Genetic programming as a means for programming computers by natural selection. *Statistics and Computing* 4(2), 87–112. <https://doi.org/10.1007/BF00175355>
- Lee, Y., Chang, S., Kim, J., Kim, I. 2024. Estimation of beach profile response on coastal hydrodynamics using LSTM-based encoder-decoder network. *Journal of Marine Science and Engineering* 12(12), 2212. <https://doi.org/10.3390/jmse12122212>
- Lesser, G.R., Roelvink, J.A., van Kester, J.T.M., Stelling, G.S. 2004. Development and validation of a three-dimensional morphological model. *Coastal Engineering* 51(8–9), 883–915. <https://doi.org/10.1016/j.coastaleng.2004.07.014>
- López, I., Aragonés, L., Villacampa, Y., Compañ, P. 2017. Artificial neural network modeling of cross-shore profile on sand beaches: The coast of the province of Valencia (Spain). *Marine Georesources & Geotechnology* 36(6), 698–708. <https://doi.org/10.1080/1064119X.2017.1385666>
- Masselink, G., Hughes, M., Knight, J. 2014. *Introduction to coastal processes and geomorphology*. Routledge, 432 pp. <https://doi.org/10.4324/9780203785461>
- Masselink, G., Scott, T., Poate, T., Russell, P., Davidson, M., Conley, D. 2016. The extreme 2013/2014 winter storms: hydrodynamic forcing and coastal response along the southwest coast of England. *Earth Surface Processes and Landforms* 41(3), 378–391. <https://doi.org/10.1002/esp.3836>
- McCall, R.T., Van Thiel de Vries, J.S.M., Plant, N.G., Van Dongeren, A.R., Roelvink, D., Thompson, D.M., Reniers, A.J.H.M. 2010. Two-dimensional time dependent hurricane overwash and erosion modeling at Santa Rosa Island. *Coastal Engineering* 57(7), 668–683. <https://doi.org/10.1016/j.coastaleng.2010.02.006>
- Meier, H.E.M., Kniebusch, M., Dieterich, C., Gröger, M., Zorita, E., Elmgren, R., Myrberg, K., Ahola, M.P., Bartosova, A., Bonsdorff, E., Börgel, F., Capell, R., Carlén, I., Carlund, T., Carstensen, J., Christensen, O.B., Dierschke, V., Frauen, C., Frederiksen, M., Gaget, E., Galatius, A., Haapala, J.J., Halkka, A., Hugelius, G., Hünicke, B., Jaagus, J., Jüssi, M., Käyhkö, J., Kirchner, N., Kjellström, E., Kulinski, K., Lehmann, A., Lindström, G., May, W., Miller, P.A., Mohrholz, V., Müller-Karulis, B., Pavón-Jordán, D., Quante, M., Reckermann, M., Rutgersson, A., Savchuk, O.P., Stendel, M., Tuomi, L., Viitasalo, M., Weisse, R., Zhang, W. 2022. Climate change in the Baltic Sea region: a summary. *Earth System Dynamic* 13, 457–593. <https://doi.org/10.5194/esd-13-457-2022>
- Murray, A.B., Gasparini, N.M., Goldstein, E.B., van der Wegen, M. 2016. Uncertainty quantification in modeling earth surface processes: more applicable for some types of models than for others. *Computers & Geosciences* 90, 6–16. <https://doi.org/10.1016/j.cageo.2016.02.008>
- Nordstrom, K.F. 2009. *Beaches and Dunes of Developed Coasts*. Cambridge University Press, 338 pp. <https://doi.org/10.1017/CBO9780511549519>
- Palmsten, M.L., Splinter, K.D., Plant, N.G., Stockdon, H.F. 2014. Probabilistic estimation of dune retreat on the Gold Coast, Australia. *Shore & Beach* 82, 35–43.
- Passeri, D.L., Hagen, S.C., Medeiros, S.C., Bilskie, M.V., Alizad, K., Wang, D. 2015. The dynamic effects of sea level rise on low-gradient coastal

- landscapes: A review. *Earth's Future* 3, 159–181. <https://doi.org/10.1002/2015EF000298>
- Plant, N.G., Stockdon, H.F. 2012. Probabilistic prediction of barrier-island response to hurricanes. *Journal of Geophysical Research: Earth Surface* 117, F03015. <https://doi.org/10.1029/2011JF002326>
- Pupienis, D., Buynevich, I., Ryabchuk, D., Jarmalavičius, D., Žilinskas, G., Fedorovič, J., Kovaleva, O., Sergeev, A., Cichoń-Pupienis, A. 2017. Spatial patterns in heavy-mineral concentrations along the Curonian Spit coast, southeastern Baltic Sea. *Estuarine, Coastal and Shelf Science* 195(5), 41–50. <https://doi.org/10.1016/j.ecss.2016.08.008>
- Roelvink, D., Reniers, A., van Dongeren, A., van Thiel de Vries, J., McCall, R., Lescinski, J. 2009. Modelling storm impacts on beaches, dunes and barrier islands. *Coastal Engineering* 56(11–12), 1133–1152. <https://doi.org/10.1016/j.coastaleng.2009.08.006>
- Ruggiero, P., Hacker, S., Seabloom, E., Zarnetske, P. 2018. The Role of Vegetation in Determining Dune Morphology, Exposure to Sea-Level Rise, and Storm-Induced Coastal Hazards: A U.S. Pacific Northwest Perspective. In: Moore, L., Murray, A. (eds) *Barrier Dynamics and Response to Changing Climate*. Springer, Cham. https://doi.org/10.1007/978-3-319-68086-6_11
- Shiri, F.M., Perumal, T., Mustapha, N., Mohamed, R. 2024. A comprehensive overview and comparative analysis on deep learning models: CNN, RNN, LSTM, GRU. *Journal on Artificial Intelligence* 6(1), 301–360. <https://doi.org/10.32604/jai.2024.054314>
- Smagulova, K., James, A.P. 2019. A survey on LSTM memristive neural network architectures and applications. *The European Physical Journal Special Topics* 228(10), 2313–2324. <https://doi.org/10.1140/epjst/e2019-900046-x>
- Soomere, T. 2023. Numerical simulations of wave climate in the Baltic Sea: a review. *Oceanologia* 65(1), 117–140. <https://doi.org/10.1016/j.oceano.2022.01.004>
- Soomere, T., Eelsalu, M., Viigand, K., Giudici, A. 2024. Linking changes in the directional distribution of moderate and strong winds with changes in wave properties in the eastern Baltic proper. *Journal of Coastal Research* 113(SI), 190–194. <https://doi.org/10.2112/JCR-SI113-038.1>
- Splinter, K.D., Turner, I.L., Davidson, M., Barnard, P.L., Castle, B., Oltman-Shay, J. 2014. A generalized equilibrium model for predicting daily to interannual shoreline response. *Journal of Geophysical Research: Earth Surface* 119(9), 1936–1958. <https://doi.org/10.1002/2014JF003106>
- Van Houdt, G., Mosquera, C., Nápoles, G. 2020. A review on the long short-term memory model. *Artificial Intelligence Review* 53(8), 5929–5955. <https://doi.org/10.1007/s10462-020-09838-1>
- van Verseveld, H.C.W., Van Dongeren, A.R., Plant, N.G., Jäger, W.S., Den Heijer, C. 2015. Modelling multi-hazard hurricane damages on an urbanized coast with a Bayesian network approach. *Coastal Engineering* 103, 1–14. <https://doi.org/10.1016/j.coastaleng.2015.05.006>
- Vellinga, P. 1986. Beach and dune erosion during storm surges. *Coastal Engineering* 10(2), 121–145. [https://doi.org/10.1016/0378-3839\(82\)90007-2](https://doi.org/10.1016/0378-3839(82)90007-2)
- Vousdoukas, M.I., Ranasinghe, R., Mentaschi, L., Plomaritis, T.A., Athanasiou, P., Luijendijk, A., Feyen, L. 2020. Sandy coastlines under threat of erosion. *Nature Climate Change* 10, 260–263. <https://doi.org/10.1038/s41558-020-0697-0>
- Weerakody, P.B., Wong, K.W., Wang, G., Ela, W. 2021. A review of irregular time series data handling with gated recurrent neural networks. *Neurocomputing* 441, 161–178. <https://doi.org/10.1016/j.neucom.2021.02.046>
- Wen, X., Li, W. 2023. Time series prediction based on LSTM-attention-LSTM model. *IEEE access* 11, 48322–48331. <https://doi.org/10.1109/ACCESS.2023.3276628>
- Wise, R.A., Smith, S.J., Larson, M. 1996. SBEACH: Numerical Model for Simulating Storm-Induced Beach Change. *Report 4. Cross-Shore Transport under Random Waves and Model Validation with SUPERTANK and Field Data* (No. CERC899).
- Zarnetske, P.L., Ruggiero, P., Seabloom, E.W., Hacker, S.D. 2015. Coastal foredune evolution: the relative influence of vegetation and sand supply in the US Pacific Northwest. *Journal of the Royal Society Interface* 12(106), 20150017. <https://doi.org/10.1098/rsif.2015.0017>